Neuron, Vol. 28, 337–348, May, 2000, Copyright ©2000 by Cell Press

Drosophila Futsch/22C10 Is a MAP1B-like Protein Required for Dendritic and Axonal Development

Thomas Hummel,* Karin Krukkert,* Jack Roos,† Graeme Davis,† and Christian Klämbt*‡
*Institut für Neurobiologie
Universität Münster
Badestr. 9
D-48149 Münster
Germany
†Department of Biochemistry and Biophysics
University of California, San Francisco
San Francisco, California 94143

Summary

Here we report the description of the *Drosophila* gene *futsch*, which encodes a protein recognized by the monoclonal antibody 22C10 that has been widely used to visualize neuronal morphology and axonal projections. The Futsch protein is 5327 amino acids in length. It localizes to the microtubule compartment of the cell and associates with microtubules in vitro. The N- and C-terminal domains of Futsch are homologous to the vertebrate MAP1B microtubule-associated protein. The central domain of the Futsch protein is highly repetitive and shows sequence similarity to neurofilament proteins of which no *Drosophila* homologs have been reported. Loss-of-function analyses demonstrate that during embryogenesis Futsch is necessary for dendritic and axonal growth. Gain-of-function analyses demonstrate a functional interaction of Futsch with other MAPs. In addition, we show that during development, *futsch* expression is negatively regulated in nonneuronal tissues.

Introduction

A typical neuron shows a remarkable architecture, with dendrites collecting and integrating neuronal activity and axons transmitting it over often long distances through the body. Neuronal cell morphology requires a precisely regulated cytoskeleton, comprising intermediate filaments, F-actin, and microtubule fibers. In the axon, microtubules are organized in a polar fashion, with the plus end always pointing to the synapse, whereas in the dendrites, both orientations can be found (Baas et al., 1988). The regulation of microtubule dynamics depends on a large group of microtubule-associated proteins (MAPs) that have been classified into three classes (Matus, 1991; Schoenfeld and Obar, 1994). The low molecular weight group of MAPs comprises kinesin-type proteins, dynamin, MAP2c, and tau. The intermediate group comprises the MAP3 and MAP4 proteins. The high molecular weight MAPs are MAP1A, MAP1B, MAP2, and cytoplasmic dynein (Schoenfeld and Obar, 1994).

‡To whom correspondence should be addressed (e-mail: klaembt@mail.uni-muenster.de).

A role for the nonmotor MAPs in the establishment of neuronal cell shape has been deduced from their distinct association with different neuronal cell compartments. MAP2 is preferentially found in dendrites and neuronal somata (Matus et al., 1981; Matus, 1991). In contrast, tau is localized in axons (Binder et al., 1985; Peng et al., 1986; Dotti et al., 1987). The MAP1 proteins are found in dendrites, somata, and axons. The correlation of MAP expression and axonal growth in developing as well as in regenerating nerves suggests a role in axonal extension (Dotti et al., 1987; Kosik and Finch, 1987; Tonge et al., 1996; Gordon-Weeks and Fischer, 2000). First evidence supporting this assumption stems from antisense experiments. Antisense RNA directed against *tau* blocks axonal outgrowth in cultured neurons (Caceres and Kosik, 1990; Caceres et al., 1991). Similarly, depletion of MAP1B or MAP2 RNA by antisense RNA or by intracellular delivery of specific antibodies resulted in reduction or inhibition of neurite outgrowth in cultured cells (Caceres et al., 1992; Brugg et al., 1993; Shea et al., 1994; DiTella et al., 1996). The unilateral ablation of phosphorylated MAP1B in growth cones using microscale chromophore-assisted laser inactivation (micro-CALI) induced changes in growth direction (Mack et al., 2000). The results indicate a functional role for P1-MAP1B in local growth cone stabilization and thus growth cone steering. However, the in vivo function of the MAPs during neuronal development is not yet clear. Neurons from a *tau* knockout mouse show normal axonal extension (Harada et al., 1994). Recently, two MAP1B knockouts in mice were reported (Edelmann et al., 1996; Takei et al., 1997). Whereas Edelmann et al. reported severe developmental defects, Takei et al. showed that mice lacking MAP1B developed into fertile adults with only a mild reduction in brain size.

In *Drosophila*, several microtubule-associated proteins have been described. Motor proteins have been analyzed most extensively (Saxton et al., 1991; Hurd and Saxton, 1996; Phillis et al., 1996; Gindhart et al., 1998; Hirokawa, 1998). Although some nonmotor MAPs have been identified in *Drosophila*, their function during neuronal development remains elusive. The *Drosophila* gene encoding the intermediate 205K MAP related to MAP4 is the best-studied example (Goldstein et al., 1986; Irminger-Finger et al., 1990). Genetic analyses have shown that the 205K MAP gene is not essential for development (Pereira et al., 1992). In addition, several other MAPs, including a tau-like MAP, have been identified biochemically (Wandosell and Avila, 1987; Alcantara et al., 1995; Cambiazo et al., 1995). Interestingly, antibodies raised against the *Drosophila* MAPs frequently cross-react with vertebrate MAP proteins (Pereira et al., 1992; Srinivasan and Karr, 1995). In addition, bovine-tau-β-galactosidase axon-targeted reporters proved to be useful tools for the analysis of the *Drosophila* nervous system (Callahan and Thomas, 1994; Ito et al., 1997; Tissot et al., 1997). Thus, proteins and mechanisms controlling microtubule assembly and stability will likely be conserved between *Drosophila* and vertebrates.

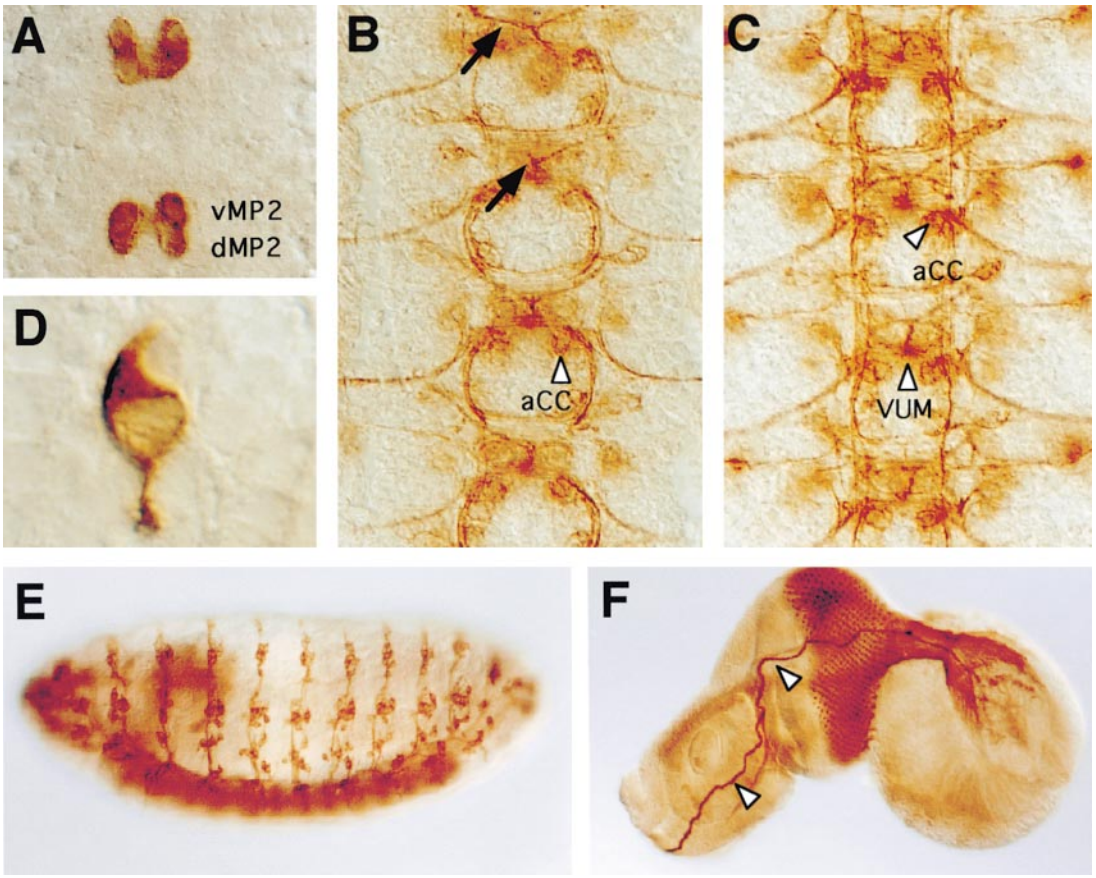

Figure 1. Expression of the 22C10 Antigen

(A–C) Frontal views of dissected embryonic CNS preparations; (D) PNS preparation; (E) stage 16 whole-mount embryo, anterior is to the left; (F) antenna-eye disc and adhering brain hemisphere. Neuronal cell bodies and axons are highlighted using the mAb 22C10 and subsequent HRP immunohistochemistry.

(A) First 22C10 expression can be detected in stage 11 embryos in the CNS. Both the dMP2 and the vMP2 cells are labeled prior to axonogenesis.

(B) At stage 13, additional neuronal cell bodies as well as their axonal trajectories express the 22C10 antigen. The arrows indicate the VUM axons that originate in the midline and bifurcate at the anterior commissure. The aCC motoneuron is indicated by an arrowhead.

(C) The distribution of the 22C10 antigen in a stage 16 embryo. The aCC motoneuron is indicated.

(D) Within the PNS, 22C10 expression can be detected shortly before axonogenesis starts. The figure shows a single PNS neuron in a stage 14 embryo. Within the developing neurons, expression of the 22C10 antigen is found in the cell soma, in the growing axon, as well as in dendritic processes.

(E) In a stage 16 whole-mount embryo, all sensory neurons express the 22C10 antigen.

(F) All developing photoreceptor neurons express the 22C10 antigen in a third instar eye disc. In addition, high levels of 22C10 expression can be found in the Bolwig nerve (arrowheads).

Here we describe the identification of the *Drosophila futsch* gene encoding a novel type of microtubule-associated protein. The Futsch protein is recognized by the long-known mAb 22C10, identified in the lab of Seymor Benzer (Fujita et al., 1982; Zipursky et al., 1984). The 22C10 antigen is expressed by some CNS neurons as well as by all neurons in the PNS. The antigen is found in all cellular compartments, the dendrite, the soma, and the axon, where it is associated with the axonal cytoskeleton (Estes et al., 1996; Roos et al., 2000 [this issue of *Neuron*]). Several noncomplementing mutations affecting the expression of the 22C10 antigen were identified. Genetic analyses demonstrate that *futsch* is necessary for axonal growth and dendritic morphology. The deduced Futsch protein is 5327 amino acids in length. The N- and C-terminal domains of Futsch are homologous to the vertebrate MAP1B, whereas the central domain of the Futsch protein is highly repetitive. Futsch localizes to the microtubule compartment of the cell and can be precipitated with taxol-stabilized bovine microtubules in vitro. Thus, *futsch* encodes a novel cytoskeletal protein.

Results

Expression of the 22C10 Antigen during Development

In *Drosophila*, the mAb 22C10 has been widely used to label neuronal cells within the PNS and CNS (Fujita et al., 1982; Canal and Ferrús, 1986; Figure 1). In all stages of development, the 22C10 antigen expression starts in postmitotic neurons shortly before axonogenesis is initiated. In the embryonic nervous system, first mAb 22C10 reactivity is detected in the MP2 neurons (Figure

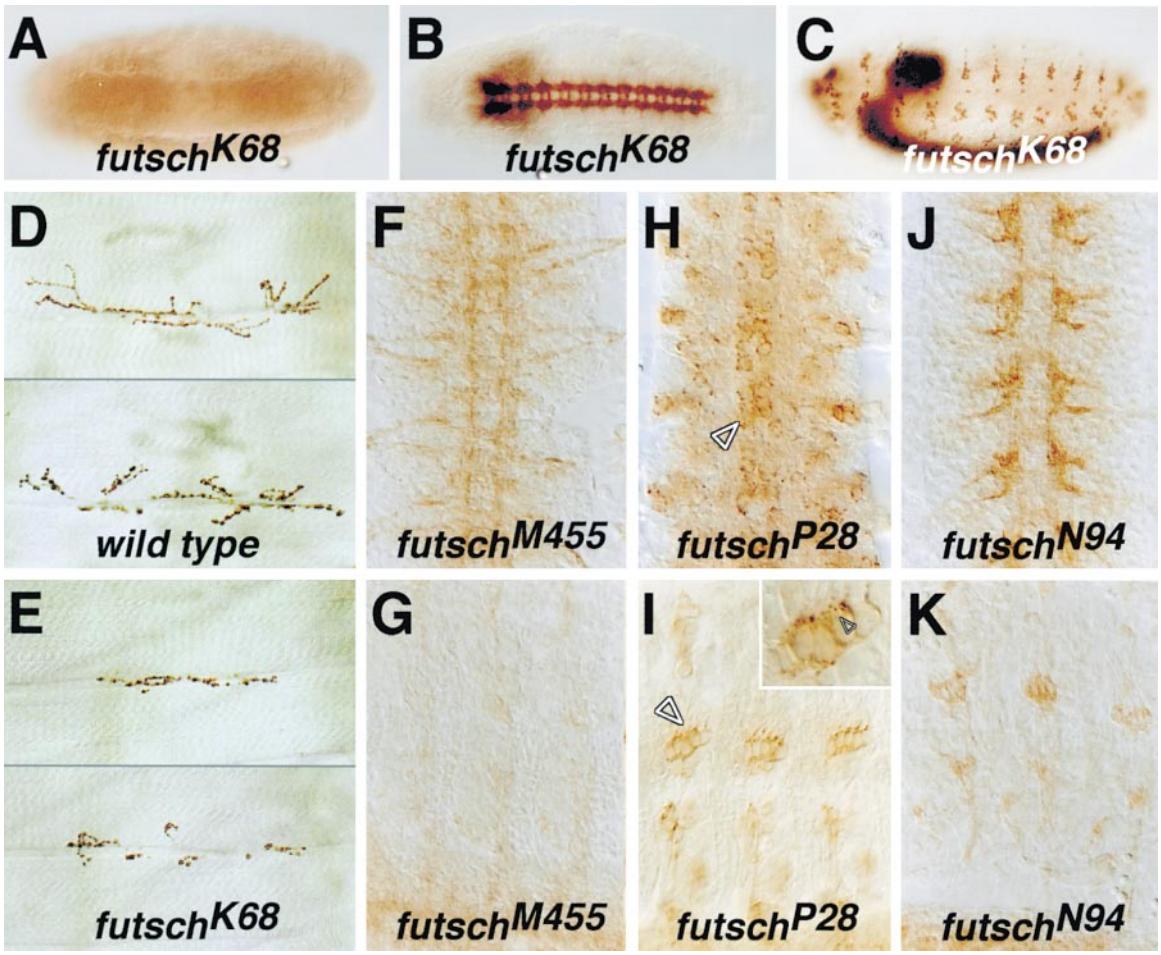

Figure 2. Mutations Affecting the Expression of the 22C10 Antigen

(A–C) Whole-mount stage 16 embryos; (D and E) preparations of the larval neuromuscular junction at muscles 6/7; (F, H, and J) frontal views of dissected stage 16 embryonic CNS preparations; (G, I, and K) stage 16 PNS preparations. The embryos were stained using mAbs 22C10 (A and F–K), BP102 (B), anti-elav (C), nc46 (D and E), and subsequent HRP immunohistochemistry.

(A) In *futsch*^{K68} embryos, no 22C10 expression can be detected.

(B) The loss of 22C10 expression does not interfere with formation of the regular ladder-like embryonic CNS axon pattern.

(C) Similarly, the expression of the neuronal antigen ELAV is not affected.

(D) In wild-type larvae, the synaptic protein NC46 is detected in many synaptic buttons.

(E) In mutant *futsch*^{K68} larvae, fewer boutons express NC46.

(F and G) The mutation *futsch*^{M455} leads to greatly reduced expression levels of the 22C10 antigen.

(H and I) In *futsch*^{P28} embryos, the 22C10 antigen is concentrated in granules in CNS as well as in PNS neurons (arrowheads, see enlargement in I).

(J) In *futsch*^{N94} embryos, expression of the 22C10 antigen is greatly reduced.

(K) In addition, subcellular localization of the Futsch protein is altered and is found preferentially at the nerve termini.

1A). During subsequent development, several interneurons and motoneurons express the 22C10 antigen (Figures 1B and 1C). Within the developing PNS, neuronal cells express the 22C10 antigen from early stages of neuronal differentiation onward. It is important to note that the 22C10 epitope is found in the growing axon, the cell body, and the dendrite (Figure 1D). At the end of embryogenesis, 22C10 expression can be found in all sensory neurons (Figure 1E). During late larval development, expression is found in all photoreceptor neurons (Figure 1F). Beside expression in the nervous system, some 22C10 antigen can be detected in the muscle attachment sites of the ventrolateral musculature (Giesen et al., 1997) and the tip cell of the malphigian tubules (Hoch et al., 1994). By using confocal microscopy, we localized the 22C10 epitope in the central axonal compartment of larval neurons associated with the microtubule cytoskeleton (see below; Estes et al., 1996; Roos et al., 2000).

Identification of the *futsch* Gene

In a large-scale EMS mutagenesis, we identified five noncomplementing X-chromosomal mutations that strongly reduce or eliminate the 22C10 antigen expression (see below). The corresponding gene maps to the interval 1F/2A on the X chromosome and was termed *futsch* (German for “gone”; see Experimental Procedures for details).

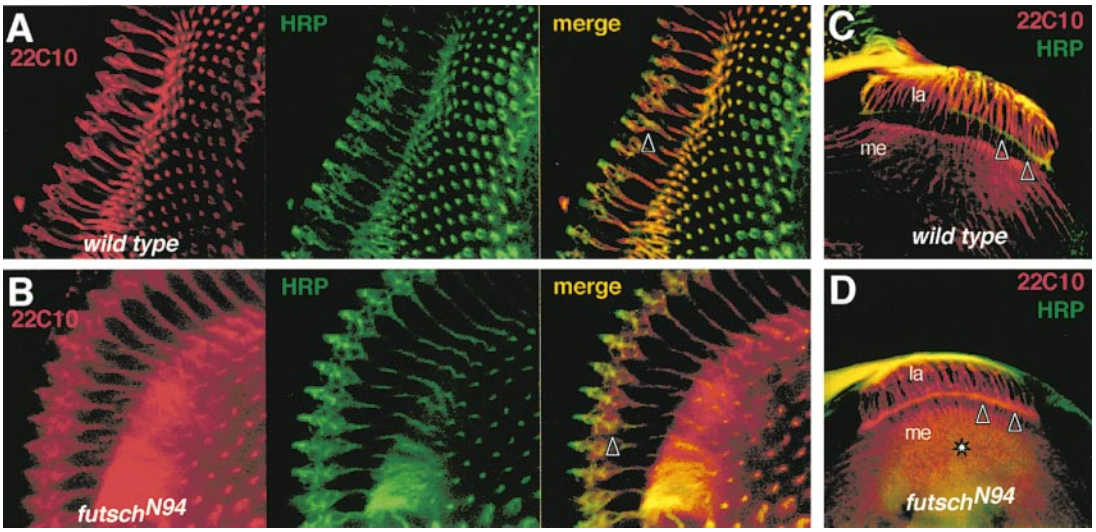

Figure 3. *futsch*^{N94} Affects the Subcellular Localization of the 22C10 Antigen

Confocal images of third instar eye discs (A and B) and larval brains (C and D). All preparations are stained using mAb 22C10 and anti-HRP antibodies.

(A) In wild-type third instar eye discs, the Futsch protein (red) is found in distinct fibers in the developing photoreceptor cells. The morphology of the photoreceptor cells is outlined by anti-HRP staining (green).

(B) In mutant *futsch*^{N94} photoreceptor cells, reduced levels of Futsch protein are evenly distributed throughout the cells. The morphology of the photoreceptor cells appears unchanged in mutant *futsch*^{N94} larvae.

(C) In wild-type larval brains, axons of the photoreceptor neurons R1–R6 terminate in the lamina (la), whereas photoreceptor axon R7 and R8 terminate in the medulla (me). Anti-HRP staining allows visualization of the termination zone of the R1–R6 axons in the lamina (arrowheads). No Futsch protein is found in the nerve termini.

(D) In *futsch*^{N94} mutant larvae, Futsch appears abundantly expressed in the growth cones of photoreceptor cells R1–R6 (arrowheads) and R7 and R8 (asterisk).

Three *futsch* mutations lead to a pronounced reduction in the level of 22C10 antigen expression including *futsch*^{M455}, *futsch*^{P28}, and *futsch*^{N94} (Figure 2). The *futsch*^{M455} allele leads to a uniform reduction in expression, while both *futsch*^{P28} and *futsch*^{N94} also lead to an abnormal subcellular distribution of Futsch. In *futsch*^{P28}, we observe a granular expression in the cell body and dendrites. Interestingly, in *futsch*^{N94}, there is diffuse staining within the nerve terminal that is not observed in wild type (Figures 2J, 3C, and 3D). We analyzed this aspect of the phenotype in the visual system. In third instar wild-type photoreceptor cells, distinct 22C10-positive fibers extend from the cell body into the axon and dendrites, but no staining is observed in the nerve terminals (Figure 3). In *futsch*^{N94}, Futsch protein is distributed uniformly in the nerve terminal (Figure 3D). The mislocalization of the Futsch protein can be clearly seen in the nerve terminals in the lamina where the photoreceptor axons of cells R1–R6 terminate as well as in the growth cones of photoreceptor cells R7 and R8 in the medulla (Figure 3D, asterisk).

In addition, *futsch*^{N94} mutant larvae show ectopic Futsch expression in the so-called optic lobe pioneer cells (OLPs; Tix et al., 1989; data not shown). Given the above data, localization of Futsch to the OLPs results from mislocalisation of Futsch to synaptic endings (see Roos et al., 2000).

futsch Is Required for Axonal and Dendritic Growth

In two mutations, *futsch*^{K68} (Figure 2A) and *futsch*^{P158} (see below), 22C10 antigen expression is eliminated. Homozygous *futsch*^{K68} flies are viable, and overall neuronal development proceeds normally in the embryo (Figures 2B and 2C). In the larvae, we noted a reduced number of synaptic boutons visualized by the antibody nc46 (Reichmuth et al., 1995) (Figures 2D and 2E; see Roos et al. [2000] for details).

In *futsch*^{P158}, we failed to separate the lethality and the absence of 22C10 expression by recombination. In wild-type embryos, highest levels of mAb 22C10 reactivity is seen in all PNS neurons. Futsch is prominently expressed in the dendrites of the five lateral chordotonal organs (lchO; Figure 4A, arrow). To analyze the morphology of the PNS neurons in mutant *futsch*^{P158} embryos, we used the GAL4 driver line *P0163* to express the transmembrane protein CD2 specifically in PNS neurons, thereby visualizing their axonal and dendritic morphology (Figures 4B and 4C). In mutant *futsch*^{P158} larvae, about 97% of the PNS neurons fail to develop their normal dendritic morphology (Figures 4D and 4E). Occasionally, however, we detected dendritic processes (Figure 4E, arrowhead, 7 dendrites in 260 lch neurons analyzed). Axonal growth is impaired as well, and few axons grew normally into the CNS (Figure 4F). Axonal pathfinding is not affected, and axons appeared to simply stop growing after some distance (Figures 4D–4F, arrowheads).

Within the ventral nerve cord, Futsch is expressed in many inter- and motoneurons that also express the Fasciclin II protein (Fas II) (van Vactor et al., 1993; Figures 4G and 4J). In stage 16 *futsch*^{P158} mutant embryos, the longitudinal connectives are reduced (Figure 4H; 100% penetrant, $>$100 embryos analyzed). Similarly, we observed disruptions in the motoneuronal connections. In

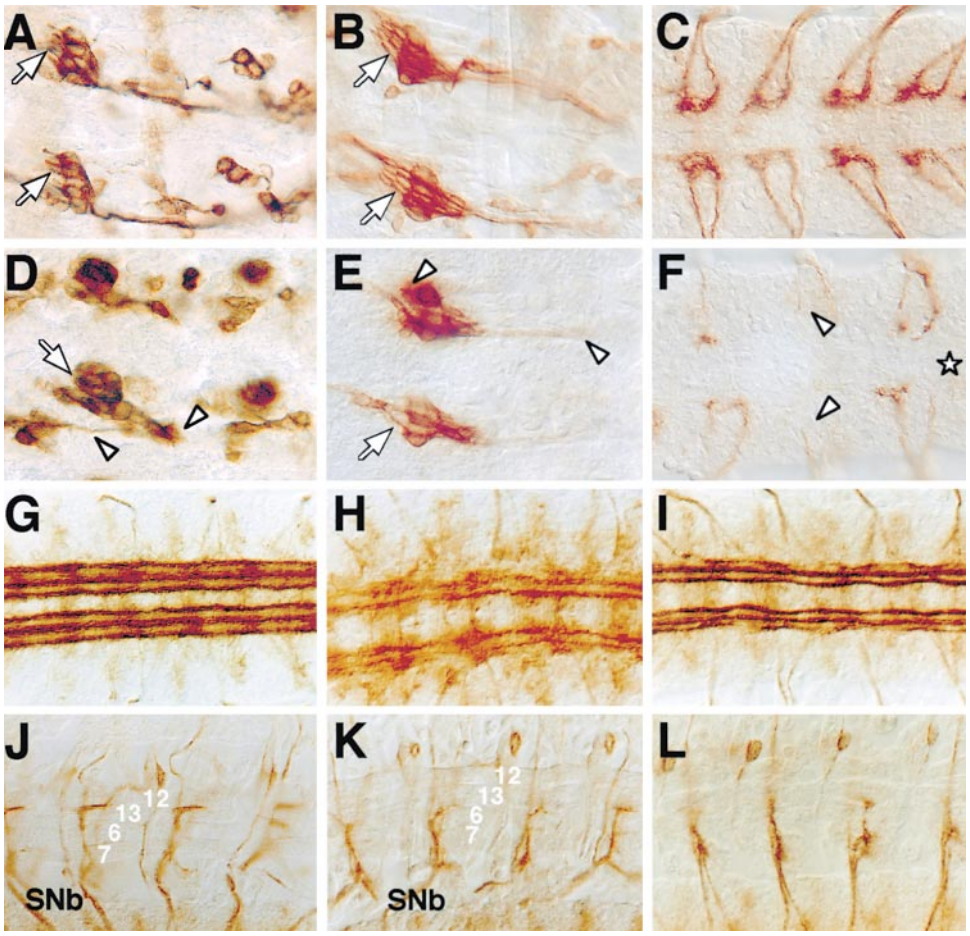

Figure 4. The Embryonic Phenotype of *futsch*^{P158}

Frontal views of dissected stage 16/17 embryonic PNS (A, B, D, E, and J–L) and CNS (C and F–I) preparations labeled with mAb 22C10 (A), anti-CD2 (B–F), or anti–Fas II antibodies (G–L) and subsequent HRP immunohistochemistry.

(A) In wild-type embryos, the mAb 22C10 antigen is found in axons, somata, and dendrites (arrow) of all sensory neurons.

(B–F) In embryos carrying the *P0163* GAL4 insertion and the *UAS-CD2* transgene, the CD2 protein is found specifically in sensory neurons.

(B) In wild-type embryos, dendritic processes (arrow) are labeled; in the lateral chordotonal organ, five dendrites can be recognized.

(C) Within the CNS CD2, reactivity is detected in the axon terminals of the sensory neurons.

(D–F) In mutant *futsch*^{P158} embryos, dendrites only rarely form. The arrows point to positions where dendrites should have formed. Sensory axons often stall (arrowheads).

(F) Only few sensory axons grow into the CNS, where they can terminate prematurely (arrowhead) or fail to develop their typical nerve terminals (asterisk).

(G) In wild-type embryos, few fascicles in the longitudinal connectives expresses Fas II.

(H) *futsch*^{P158} mutant embryos show abnormal longitudinal connectives. The lateral-most Fas II–positive fascicle is not formed properly.

(I) A similar Fas II phenotype is found in *Df(1)AC7* embryos.

(J) In wild-type embryos, motoaxons exit the CNS via the segmental and intersegmental nerve and innervate the somatic musculature (numbers indicate different muscle fibers).

(K) In mutant *futsch*^{P158} embryos, the motoaxons fail to reach their target muscles, and a short stop–like phenotype develops.

(L) A similar phenotype is found in *Df(1)AC7* embryos.

particular, SNb nerves fail to reach muscle fibers 12 and 13 (Figure 4K). Motoneurons stall and fail to set up the correct innervation pattern in 89% of the segments (58 of 65 segments; in 7 segments, more severe phenotypes were observed). To determine the null phenotype of *futsch*, we analyzed the CNS defects associated with the deficiencies *Df(1)A94* and *Df(1)S39* that remove the *futsch* locus. In both cases, we observed a nervous system phenotype very similar to the *futsch*^{P158} mutant phenotype (Figures 4I and 4L). Thus, *P158* appears to be an amorphic mutation, whereas the *K68* is a hypomorphic mutation of the *futsch* gene. Loss of *futsch* function leads to disruption of dendritic and axonal growth.

futsch Encodes a Large Protein

In order to determine the size of the Futsch protein, we separated wild-type proteins on 4% SDS-PAGE gels. The equivalent of four heads was loaded on each lane (Figure 5A). Following Western blot analysis, the size of the Futsch protein was estimated to be >500 kDa (Figure 5A). In wild-type extracts, generally a prominent large protein with an apparent molecular weight >500 kDa reacted with the mAb 22C10. In homozygous mutant

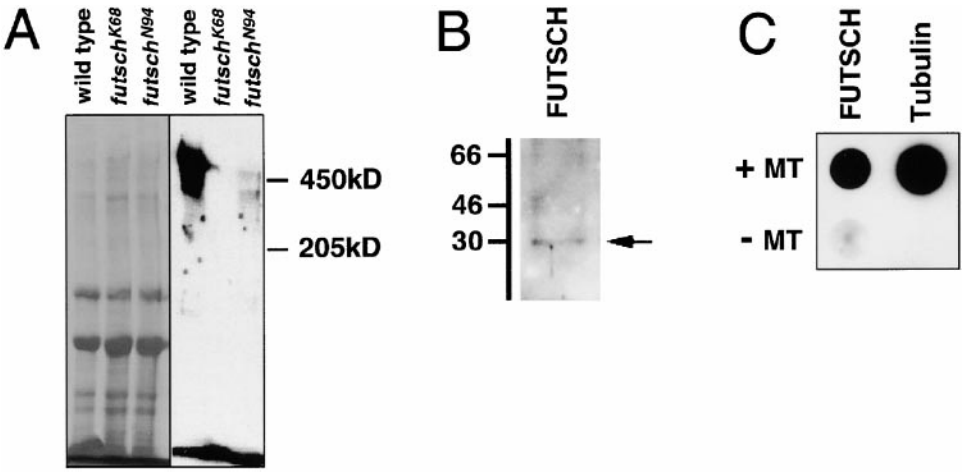

Figure 5. In Vitro Analysis of Futsch

(A) MAb 22C10 recognizes the Futsch protein. Extracts from wild-type and the hypomorphic *futsch* mutants (*futsch*^{K68} and *futsch*^{N94}) were resolved on a 4% SDS-PAGE gel and immunoblotted for the presence of Futsch. A Coomassie blue–stained gel is shown to demonstrate equivalent loading between the genotypes. The 22C10 monoclonal antibody recognizes a protein band of >500 kDa present in wild-type extracts; the presence of Futsch is not detected in the *futsch*^{K68} hypomorphic background and is greatly reduced in the *futsch*^{N94} hypomorphic background. In addition, the size of the Futsch^{N94} protein appears reduced.

(B) The 22C10 antibody reacts to an antigen that is localized to the C terminus of Futsch. Mild acid hydrolysis was used to proteolyze the Futsch protein. Ten percent acetic acid hydrolysis will cleave Futsch at aspartyl-prolyl bonds, generating peptides of molecular weight (in kDa) 260, 89, 86, 38, 34, 31, 25, and 12. A 31 kDa product was detected by Western blot analysis, corresponding to amino acids 4685–4982 (indicated in Figure 7A).

(C) Futsch precipitates in a complex with bovine microtubules. Microtubules were polymerized as described and added to supernatant enriched for Futsch. Binding reactions were pelleted through a 60% glycerol cushion, pellets were resuspended, and equal volumes were assayed by dot blot for the ability of Futsch to coprecipitate with microtubules. Coprecipitation of Futsch with microtubules was not due to trapping as judged by analysis of Sy pro-stained gels from microtubule pull-down experiments.

futsch^{K68} heads, we failed to detect any protein demonstrating the specificity of the antibody. In *futsch*^{N94} mutant heads, reduced levels of Futsch protein were detected, similar to what had been observed following antibody staining of *futsch*^{N94} mutant embryos (Figures 2J, 2K, and 5A). In addition, the Futsch^{N94} protein appeared to have a reduced molecular weight.

Molecular Analysis of the *futsch* Gene

In *Drosophila*, modified P elements called EP elements have been generated that contain UAS sequences in their 3′ region. EP elements oriented 5′-3′ upstream of an endogenous gene can induce the overexpression of the downstream gene in the presence of a tissue-specific source of GAL4 (Rorth, 1996; Rorth et al., 1998). *futsch* was mapped genetically to the interval 1F2A on the X chromosome. Within this interval localizes the EP element insertion *EP(X)1419* (Berkeley *Drosophila* Genome Project, BDGP). We crossed *EP(X)1419* to several GAL4 lines with known tissue-specific expression patterns and always observed a corresponding ectopic expression of the 22C10 antigen (Figure 6A). Ectopic expression occurred in the same temporal sequence as *UAS-lacZ*-directed β-galactosidase expression, indicating a direct effect of the *EP(X)1419* insertion on the level of 22C10 expression. These ectopic expression experiments also suggest that the insertion *EP(X)1419* is located upstream of the *futsch* gene.

The first predicted ORF downstream of the *EP(X)1419* insertion encodes a large protein of 5327 amino acids that matches the size of the Futsch protein as determined by Western blot analysis. Furthermore, RNA expression of this large ORF resembles the 22C10 expression pattern, consistent with this ORF representing the 22C10 antigen (data not shown; see Figure 7 for probes used).

To obtain further support that *futsch* encodes the 22C10 antigen, we analyzed *futsch* expression in mutant backgrounds that specifically alter the 22C10 expression pattern. The Zn finger transcription factor Tramtrack acts as a repressor of 22C10 antigen expression, and in *tramtrack* mutant embryos, high levels of 22C10 antigen are found in the mesoderm (Giesen et al., 1997). Consistent with Futsch being the 22C10 antigen, the expression of *futsch* mRNA is also drastically increased in *tramtrack* mutant embryos (Figures 6C and 6D). In a second experiment, we used a *ftz-GAL4* driver line (M. Grewe and C. K., unpublished data) and *EP(X)1419* to drive ectopic *futsch* expression in a pair-rule expression pattern. Ectopic expression of the 22C10 antigen correlates with ectopic expression of the deduced *futsch* transcript (Figures 6A and 6B), further supporting that *futsch* encodes the 22C10 antigen.

Futsch Is Homologous to MAP1B and Associates with Microtubules In Vitro

The *futsch* ORF shows high homology to MAP1B and MAP1A at both the N terminus as well as at the C terminus (probability e^{-69}, using standard alignment parameters [Altschul et al., 1990]; Figures 7B and 8). However,

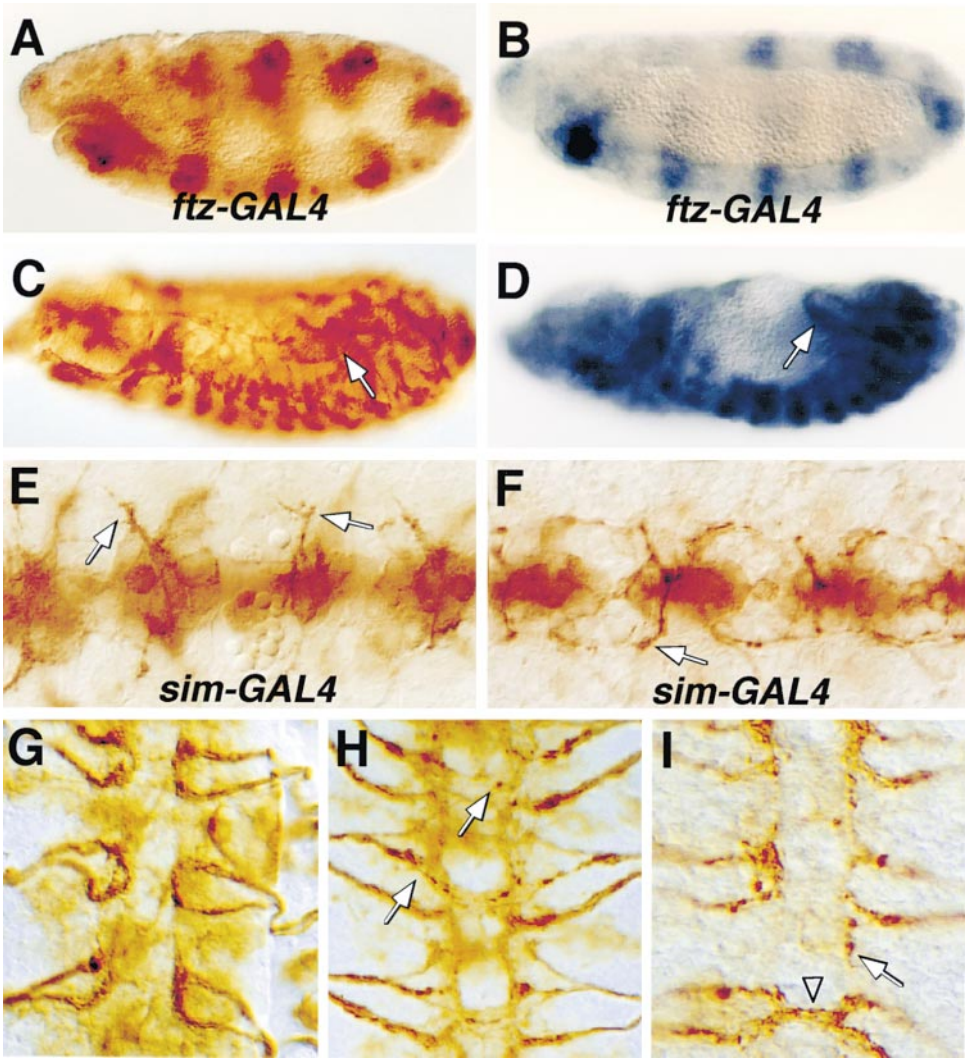

Figure 6. Ectopic Expression of *futsch* Affects Axonal Morphology

Whole-mount embryos stained for the presence of the Futsch protein (A, C, and E–I) or *futsch* RNA (B and D). The following genotypes were used: (A and B) *ftz-GAL4*, *EP(X)1419*; (E and F) *sim-GAL4*, *EP(X)1419*; (G) *44-GAL4*, *EP(X)1419*; (H and I) *44-GAL4*, *EP(X)1419 UAS-MAP2c*.

(A) Lateral view of a stage 11 embryo expressing the 22C10 antigen in a *ftz* pair-rule pattern.

(B) Similarly, the *futsch* RNA expression is found in a pair-rule pattern.

(C) In mutant *tramtrack* embryos, high levels of Futsch expression can be seen in the somatic musculature as well as in the hindgut musculature (arrow).

(D) In *tramtrack* mutant embryos, ectopic expression of *futsch* RNA is observed. Note the high levels of *futsch* expression in the hindgut (arrow).

(E and F) Frontal views of stage 12 and stage 13 CNS preparations. High levels of ectopic 22C10 expression can be seen in all midline cells.

(E) The growth cones of the MP1 neurons can be seen (arrows). They project normally; however, the growth cones have an unusual appearance, with many additional protrusions.

(F) In slightly older embryos, the VUM axons can be seen as well (arrow); they appear in close neighborhood to the MP1 axons. The appearance of individual fascicles is abnormal; however, during older stages, no defects can be seen in the organization of the general CNS axon pattern.

(G) Following overexpression of Futsch in all sensory neurons, axonal morphology appears normal.

(H and I) Coexpression of Futsch and MAP2c results in frequent axonal swellings (arrows) and misprojection phenotypes (arrowhead).

the microtubule binding domains in the N-terminal and C-terminal domains do not appear to be conserved (Noble et al., 1989; Zauner et al., 1992). The large middle domain of the deduced Futsch protein shows a highly repetitive structure. In total, 66 direct repeats of a 37 amino acid–long sequence motif are found (Figure 7C). Two blocks of 11 and 20 highly conserved units are flanked by less conserved repeat units (homology $>$40% identity). Database searches using the Futsch repeat unit revealed some homology to the neurofilament protein family (probability e^{-14}). Interestingly, the sequence KSPXXXP, which is frequently found in the Futsch repeats and in neurofilament proteins, has been described as a target of Erk2 protein kinases (Veeranna et al., 1998). Whether Futsch is phosphorylated at these positions remains to be determined.

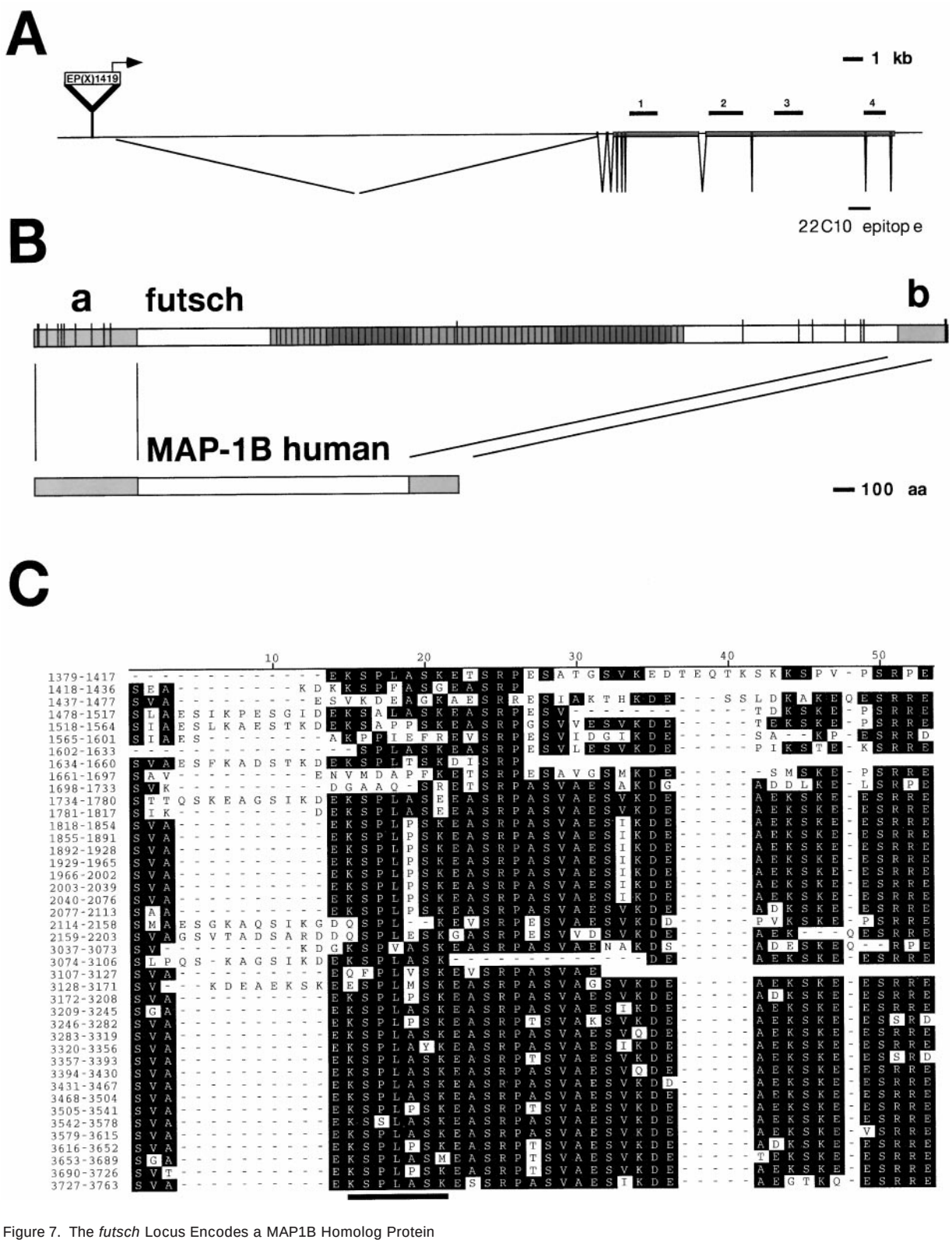

Figure 7. The *futsch* Locus Encodes a MAP1B Homolog Protein

(A) The genomic organization is indicated. All sequence information has been generated by the European *Drosophila* Genome Project. *futsch* exons are located on cosmid 49E4 (accession number AL031128). The probes used to test transcription of the predicted exons as well as the location of the 22C10 epitope are indicated.

(B) The deduced Futsch protein is 5327 amino acids in length; N- and C-terminal domains share similarity to the vertebrate MAP1B protein (Lien et al., 1994). A sequence comparison of regions designated (a) and (b) is shown in more detail in Figure 8. The middle part of the Futsch protein is composed of 60 direct repeats of a 37 amino acid–long domain. The level of shading indicates the degree of sequence identity. The small vertical bars indicate cysteine residues that are found almost exclusively at the protein termini.

(C) Forty-two repeat units are shown; the numbers indicate the position within the deduced Futsch protein. Seventeen repeat units from the middle part of the protein were omitted. Identical amino acids are shaded in black. The KSPXXXK motif is underlined.

To further prove that the high molecular weight immunoreactive band identified by the 22C10 antibody corresponded to Futsch, fractions enriched in Futsch were subjected to mild acid hydrolysis (Landon, 1977). This procedure cleaves polypeptides at aspartyl-prolyl bonds. There are seven such bonds in the deduced Futsch protein. This treatment will generate eight predicted peptide fragments of the molecular weights (in kDa) 260, 89, 86, 38, 34, 31, 25, and 12. Immunoblot analysis of this treatment is shown in Figure 5B. The 31 kDa peptide fragment identified could represent either the 25, 31, or 34 kDa digestion products. However, the predicted 25 and 34 kDa peptides correspond to amino acids 308–542 and 1–307, respectively. Since the 22C10 antibody does not recognize a mini-Futsch expression construct that includes these amino acids, we can eliminate the 25 and 34 kDa fragments as candidates. Therefore, the epitope recognized by 22C10 has been assigned to a C-terminal domain of Futsch corresponding to amino acids 4685–4982 (Figure 7A).

Further in vitro experiments assaying for the presence of Futsch were pursued by dot blot. Adult wild-type heads were homogenized and then fractionated by differential centrifugation fractionation. Equivalent mass amounts of sample were blotted by dot blot analysis for the presence of Futsch. Futsch was absent from the 1000 × g pellet, was found in the 25,000 × g pellet, and was found in reduced concentration in the 25,000 × g supernatant. Tubulin is also present in the 25,000 × g pellet, suggesting the presence of cold-stable microtubules. Consistent with this hypothesis, we were able to enrich for Futsch in this supernatant by homogenization in 4 mM calcium that destabilizes cold-stable microtubules (data not shown). To determine if Futsch and tubulin associate in a complex, the supernatant from adult head extracts was incubated with polymerized microtubules at 37°C. Futsch was enriched in the subsequent pellet fraction in the presence of taxol-stabilized bovine microtubules (Figure 5C, +MT). Thus, Futsch cofractionates with microtubules, and soluble Futsch can be precipitated with exogenously added vertebrate microtubules to adult fly head supernatants.

Elevated *futsch* Expression

futsch is an essential gene that is required for dendritic and axonal growth. However, *futsch* is not expressed in all neurons, nor is it expressed in all tissues. Several lines of evidence support the conclusion that *futsch* expression is tightly controlled through negative regulation. We as well as others have identified a number of loci that affect the expression of the 22C10 antigen (Salzberg et al., 1994, 1997; Kania et al., 1995; T. H., K. Schimmelpfeng, and C. K., unpublished data). Among these, mutations in the Zn finger transcription factor encoded by *tramtrack* lead to an ectopic expression of the 22C10 antigen in the entire somatic and visceral musculature (Figure 6C; Giesen et al., 1997). Despite high levels of *futsch* expression, however, the morphology of the mesodermal cells appears relatively normal.

In the nervous system, elevated levels of *futsch* expression were induced using the *EP(X)1419* insertion and different GAL4 driver lines (see Experimental Procedures for details). High levels of Futsch expression lead to changes in the morphology of individual growth cones and cause minor defects in the projection of individual axons (Figures 6E and 6F, arrows). However, these early axonal phenotypes did not lead to defects in the later formation of the CNS axon pattern (data not shown).

Coexpression of Futsch with Other Microtubule-Associated Proteins Disrupts Axonal Development

Beside MAP1B, tau has been implicated in neuronal development. Because so far no mutations in tau-related proteins have been described in *Drosophila*, we used the GAL4 system to analyze the effects of over- and coexpression of Futsch with different vertebrate MAPs on axonogenesis in the embryonic PNS.

As described above, expression of high levels of Futsch in the developing nervous system does not alter axonal morphology and projection pattern (Figure 6G). Similarly, expression of tau-GFP or rat MAP2c, a tau-related protein, does not interfere with normal development (data not shown). However, coexpression of Futsch and MAP2c in all PNS neurons resulted in mislocalization of the Futsch protein. Futsch accumulated locally within the axon and led to swellings, similar to what has been observed in mutants affecting axonal transport (Figures 6H and 6I). Interestingly, in older embryos, pathfinding errors became apparent in embryos expressing Futsch and MAP2c. In 20% of the neuromeres analyzed, sensory neurons project their axons in one of the two commissures across the CNS midline and fasciculate with their contralateral counterparts, which they never do in wild-type embryos (Figure 6I). The same kind of Futsch accumulation and axonal misprojection can be seen following the coexpression of Futsch and human tau, although with a reduced penetrance compared to MAP2c (10%–15%). Thus, coexpression of Futsch and other MAPs interferes with axonal development, very likely by disrupting cytoskeleton organization in the extending neuronal processes.

Discussion

Here we describe the identification and characterization of the gene *futsch* encoding the 22C10 antigen, which has been widely used as a neuronal marker in *Drosophila* for almost 20 years. Loss of *futsch* function leads to embryonic lethality with pronounced neuronal defects. Our genetic evidence demonstrates that Futsch is necessary for normal dendritic and axonal outgrowth. *futsch* encodes a large protein that cosediments with microtubules. This is in agreement with the deduced Futsch protein sequence that shows significant homology to vertebrate microtubule-associated protein 1B (MAP1B).

We present several lines of evidence indicating that the *futsch* gene encodes the 22C10 antigen. Of all deficiencies covering about 80% of the genome, only those removing the interval 1F/2A eliminated all 22C10 antigen expression. All EMS-induced *futsch* alleles map to this interval. An *EP* insertion was found to be integrated in the presumed *futsch* 5′ regulatory region and can be used to efficiently activate 22C10 antigen expression. The first ORF downstream of this *EP* insertion is expressed during embryogenesis in a pattern that closely

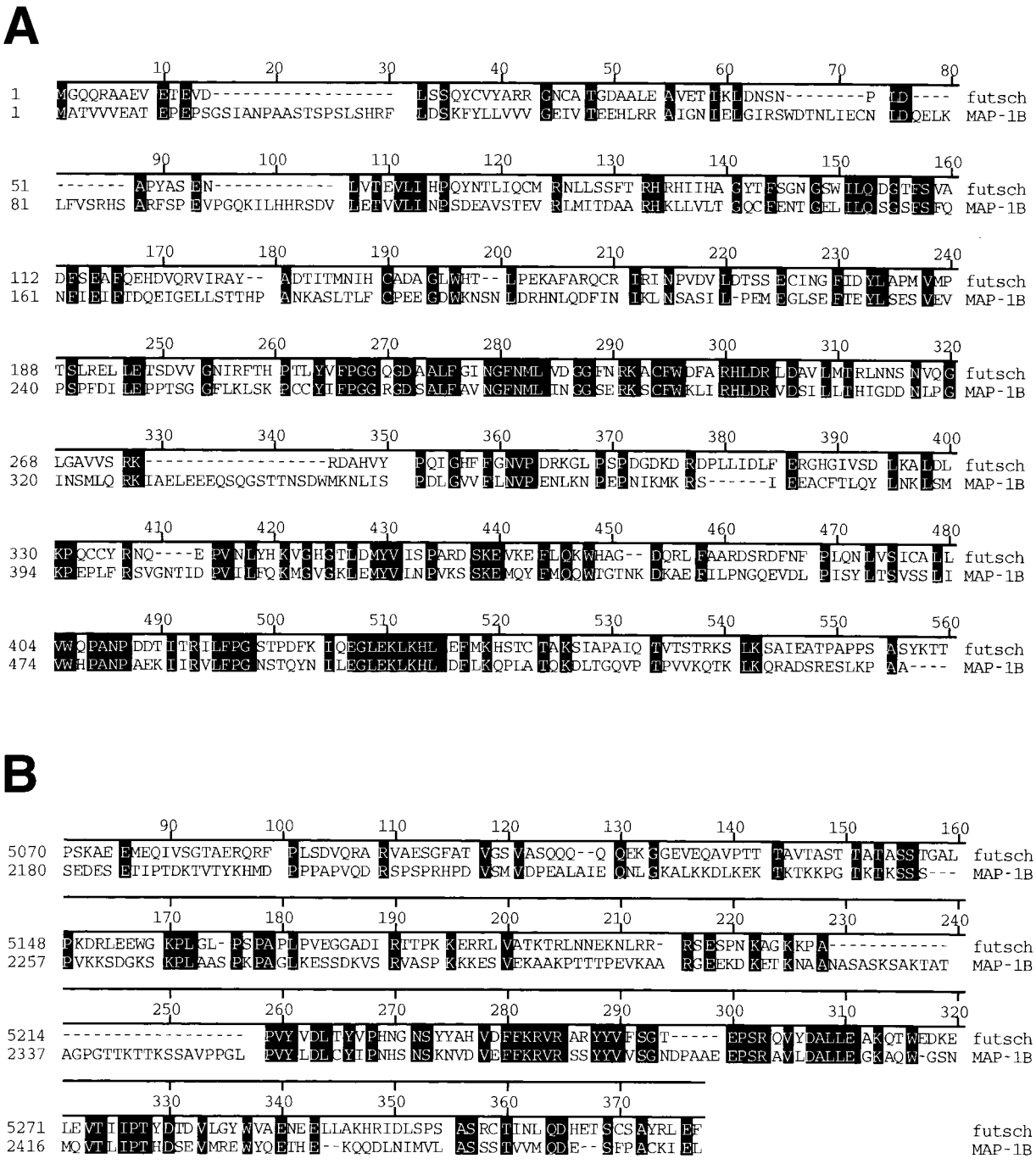

Figure 8. Sequence Comparison of Futsch and Human MAP1B N- and C-Terminal Protein Sequences

(A) shows the N-terminal 600 amino acids, and (B) shows the C-terminal 295 amino acids. Identical amino acids are shaded in black.

matches the expression pattern of the 22C10 protein. In addition, both the levels of the 22C10 antigen and the levels of *futsch* RNA expression are increased in *tramtrack* mutant embryos. The size of the Futsch protein deduced from Western blot experiments (>500 kDa) is in good agreement with the conceptual translation of the *futsch* gene (575 kDa). Furthermore, an N-terminal deletion construct is able to partially rescue the hypomorphic *futsch* mutant phenotype (Roos et al., 2000).

The deduced Futsch protein is 5327 amino acids in length and shows significant homologies to the vertebrate MAP1A and MAP1B proteins. In addition, confocal microscopy reveals that Futsch colocalizes with the microtubule cytoskeleton, strengthening the notion that Futsch interacts with the microtubule cytoskeleton (Roos et al., 2000). Furthermore, it has been shown that in *futsch*^{N94} larvae, both Futsch and the microtubule localization are disrupted, but they continue to colocalize despite altered distribution (Roos et al., 2000). Thus, colocalization experiments, in vitro analysis, as well as

genetic evidence suggest that Futsch is associated with the microtubule cytoskeleton and is necessary for microtubule organization (see Roos et al., 2000).

Beside the sequence homologies, other similarities exist between Futsch and MAP1 genes. Neuronal MAP1B expression can be induced by glial cells (Kirkpatrick and Brady, 1994). Similarly, Futsch expression is induced in the MP2 neurons by glial cells during *Drosophila* CNS development (Klaes et al., 1994). Another similarity is demonstrated by examining *futsch* RNA localization. *futsch* RNA is found in the neuronal cell somata as well as in dendritic processes (unpublished data). Similarly, MAP1A RNA has been found in dendritic processes (Schoenfeld and Obar, 1994).

The MAP1B proteins and especially the N- and C-terminal protein domains are highly conserved during vertebrate evolution (Lien et al., 1994; Kutschera et al., 1998). MAP1A and MAP1B sequences are more distantly related, and again, the strongest sequence conservation is observed at the ends of the proteins (N-terminal domain = 70%, C-terminal domain = 80% identity) (Hammarback et al., 1991; Langkopf et al., 1992; Lien et al., 1994; Fink et al., 1996). The same regions show high homology to the Futsch protein, suggesting that Futsch may represent a new member of this MAP family. MAP1B differs from MAP1A by the addition of about 220 amino acids at the N terminus. Since the homology to Futsch starts within this region, we designated Futsch as a MAP1B homolog. The microtubule binding domains identified in the N and C parts of MAP1B (Noble et al., 1989; Zauner et al., 1992) are not conserved in the Futsch protein. Although our genetic, colocalization, and in vitro data suggest a strong interaction between Futsch and the microtubule cytoskeleton, this association could be mediated either by direct or indirect binding of Futsch to the microtubules.

The highly regulated expression of phosphorylated MAP1B suggests an important function during the development of the nervous system. Blocking MAP1B expression in cultured neuronal cells inhibits neurite outgrowth (Brugg et al., 1993; DiTella et al., 1996). Furthermore, neutralization of phosphorylated MAP1B in only half of the growth cone by micro-CALI changed motility and the growth direction of the growth cone (Mack et al., 2000). These in vitro studies imply that MAP1B is essential for neuronal development and that the local concentration of MAP1B within the growth cone influences axon guidance.

MAP1B knockout experiments, however, have yielded conflicting data about the in vivo role of MAP1B. Genetic knockout data indicates that MAP1B is required for embryonic viability, and even heterozygous animals show mutant phenotypes, such as slower growth rates and motor system abnormalities (Edelmann et al., 1996). These results are very similar to the ones observed in the *Drosophila* mutation *futsch*^{P158}. The MAP1B knockout by Takei et al. (1997) did not affect all MAP1B splice variants, and residual MAP1B protein expression could still be detected (Kutschera et al., 1998). This hypomorphic MAP1B mutation resulted in homozygous viable mice with delayed nervous system development similar to the phenotype seen in mutant *futsch*^{K68} or *futsch*^{N94} animals. The MAP1B gene knockout by Edelmann et al. (1996) also resulted in a truncation of the gene leaving a 571 amino acid–long N-terminal domain intact for which a dominant-negative activity was postulated (Takei et al., 1997). To test whether expression of a similar truncated Futsch protein leads a dominant-negative phenotype, we constructed a UAS-mini-*futsch* gene encoding a comparable Futsch protein consisting of only the first 527 amino acids. High levels of expression of this protein variant did not interfere with normal development (data not shown), supporting the notion that the N-terminal domain of MAP1B has no dominant-negative effect. Rather, the N-terminal Futsch domain has weak rescuing abilities (Roos et al., 2000).

Conclusion

Here we have demonstrated that a MAP1B-like protein, *Drosophila* Futsch, is necessary for axon and dendrite growth in vivo. In a companion paper, Roos et al. (2000) demonstrate that *futsch* is necessary for the organization of the synaptic microtubule cytoskeleton and is necessary for normal synaptic growth. These data demonstrate the importance of regulated microtubule dynamics in these processes and opens up the possibility for future genetic investigations into the regulation of microtubule dynamics in *Drosophila*.

Experimental Procedures

Genetics

All *futsch* alleles were isolated in a large-scale screen for defects in the developing nervous system based on loss or alterations in the expression of the 22C10 antigen. *futsch* was mapped by recombination and deficiency mapping. The following chromosomal aberrations were used, breakpoints are indicated: *Df(1)RH4* (1A1; 1F/2A), 22C10 negative; *Df(1)S39* (1E1-2; B5), 22C10 negative; *Df(1)AC7* (1E3-4; 2A), 22C10 negative; *Dp(1,2)E1* (1A-1F), 22C10 positive. The previously published SOX2 antibody also recognizes the Futsch protein (Goodman et al., 1984). Excision mutagenesis was performed using the *Ki p*^{p} *Δ2-3* chromosome, which carries a stable source of P-transposase (Robertson et al., 1988). To analyze the PNS phenotype of mutant *futsch* embryos, we used the GAL4 driver line *P0163* (isolated in a large GAL4 enhancer trap screen performed in the labs of W. Janning and C. K. in Münster) and a *UAS-CD2* transgene (Dunin-Borkowski and Brown, 1995).

DNA Work

All probes indicated in Figure 7A were generated using primers deduced from the sequence provided by the European *Drosophila* Genome Project (EDGP). Details are available on request. Thirty PCR cycles were done: 30 s at 95°C, 30 s at 52°C, and 2 min at 75°C. A PCR product encoding the N-terminal 618 amino acids was cloned into pUAST (Brand and Perrimon, 1993) and used for germline transformation according to standard procedures. The accession number of *futsch* is CAA20006.

Protein Work

Four percent SDS-PAGE protein gels were performed according to standard procedures. Western blot transfer was done at 0.12 A for 16 hr. The gel was placed on filters soaked with 1% SDS prior to the transfer to the nitrocellulose filter. MAb 22C10 was diluted 1/200, secondary antibodies at 1/2000.

Acid Hydrolysis

0.5 mg adult head protein (25,000 × g pellet fraction) was dissolved in 100 μl Buffer A (150 mM NaCl/10 mM HEPES/1 mM EDTA/0.1 mM $MgCl_2$) plus 10% acetic acid. The reaction mixture was then incubated at 37°C for 96 hr (Landon, 1977). The reaction was terminated by neutralizing the solution with NaOH. Twenty microgram protein was analyzed on a 7%–15% SDS-PAGE gel.

Biochemical Fractionation

Adult wild-type heads (20 ml) were frozen in liquid nitrogen. The heads were pulverized in a mortar and pestle and then homogenized in 10 ml Buffer A using a Dounce homogenizer. The homogenate was then diluted with Triton X-100 to a final concentration of 1% and incubated on ice for 30 min. The extract was then centrifuged at 1000 × g for 10 min in a microcentrifuge. The resulting pellet (P1) was resuspended in an equivalent volume of Buffer A. The supernatant was then centrifuged at 25,000 × g for 30 min in a TL100 miniultracentrifuge. The resulting pellet (P2) was resuspended in 1 ml of Buffer A. Protein quantitation assays were performed on each fraction using the Pierce BCA reagent system.

Microtubule Pulldown Assays

Purified tubulin and taxol were generously supplied by S. Rice and R. Vale (University of California, San Francisco). 0.5 ml bovine tubulin (5 mg/ml) was centrifuged at 100,000 × g in a TL100 miniultracentrifuge. The supernatant was removed and placed in a fresh tube. Microtubules were polymerized by combining the supernatant, GTP (0.5 mM final concentration), and taxol (20 μM final concentration) and incubating the mixture at 37°C for 20 min. Polymerized microtubules were isolated by layering 125 μl of polymerization reaction on a 150 μl 60% glycerol/Buffer A/20 μM taxol cushion and centrifugation at 80,000 rpm for 10 min at 25°C in a TL100 miniultracentrifuge. The cushion was removed, and the pellet was quickly washed with Buffer A/20 μM taxol. The microtubule pellet was resuspended in 100 μl Buffer A/20 μM taxol. Two 1 ml aliquots of S2 supernatant (10 mg/ml) were incubated at 37°C for 30 min either in the presence (100 μl polymerized microtubules described above) or absence of microtubules. Each reaction was then layered on a 1 ml 60% glycerol/Buffer A/20 μM taxol cushion and centrifuged at 80,000 rpm for 10 min at 25°C in a TL100 miniultracentrifuge. The cushion was removed and the pellet was washed with Buffer A/20 μM taxol. The resulting pellet was resuspended in 0.5 ml 8 M urea. Protein quantitation assays were performed on each fraction using the Pierce BCA reagent system.

Misexpression Studies

Directed *futsch* gene was achieved using the *EP(1)1419* insertion or the above-described UAS-mini-*futsch* transgene and the GAL4 driver lines *sim*-GAL4 (Scholz et al., 1997), *ftz-GAL4*, and *44-GAL4* (M. Grewe and C. K., unpublished data).

Histological Methods

In situ hybridization and immunohistochemistry was performed as described (Tautz and Pfeifle, 1989; Hummel et al., 1997).

Acknowledgments

We thank S. Benzer for the monoclonal antibody 22C10; E. Buchner and C. S. Goodman for providing the mAbs nc46 and 1D4; and M. Grewe for providing flies. We also thank the EDGP and the BDGP for their efforts in sequencing the *Drosophila* genome and for making the information available to the community and for providing the *EP(X)1419* insertion line; Kathy Matthews and the Bloomington and Umea stock centers for sending us many fly strains; J. Campos-Ortega, S. Granderath, U. Lammel, J. Pielage, and K. Schimmelpfeng for help throughout the project; unknown reviewers for their encouragement to characterize the MAP properties of Futsch; and E. Rudloff, V. Gerke, S. Rice, and R. Vale for purified tubulin and taxol and technical advice. This work was supported by a Burroughs Welcome Young Investigator Award, Merck Scholar Award, seed money, a Young Investigator Grant from the Sandler Foundation, and NIH grant NS39313–01 (to G. W. D.). J. R. was supported by a Postdoctoral Fellowship T32-CA 09270–23. C. K. was supported by the Deutsche Forschungsgemeinschaft and the Human Frontiers Science Program.

Received January 27, 2000; revised April 18, 2000.

References

Alcantara, A.A., Srinivasan, S., Reilein, A.R., and Karr, T.L. (1995). Antibodies directed against microtubule proteins from Drosophila melanogaster cross react with similar proteins in the rat brain. Brain Res. *701*, 47–54.

Altschul, S.F., Gish, W., Miller, W., Myers, E.W., and Lipman, D.J. (1990). Basic local alignment search tool. J. Mol. Biol. *215*, 403–410.

Baas, P.W., Deitch, J.S., Black, M.M., and Banker, G.A. (1988). Polarity orientation of microtubules in hippocampal neurons: uniformity in the axon and nonuniformity in the dendrite. Proc. Natl. Acad. Sci. USA *85*, 8335–8339.

Binder, L.I., Frankfurter, A., and Rebhun, L.I. (1985). The distribution of tau in the mammalian central nervous system. J. Cell Biol. *101*, 1371–1378.

Brand, A.H., and Perrimon, N. (1993). Targeted gene expression as a means of altering cell fates and generating dominant phenotypes. Development *118*, 401–415.

Brugg, B., Reddy, D., and Matus, A. (1993). Attenuation of microtubule associated protein 1B expression by antisense oligodeoxynucleotides inhibits initiation of neurite outgrowth. Neuroscience *52*, 489–496.

Caceres, A., and Kosik, K.S. (1990). Inhibition of neurite polarity by tau antisense oligonucleotides in primary cerebellar neurons. Nature *343*, 461–463.

Caceres, A., Potrebic, S., and Kosik, K.S. (1991). The effect of tau antisense oligonucleotides on neurite formation of cultured cerebellar macroneurons. J. Neurosci. *11*, 1515–1523.

Caceres, A., Mautino, J., and Kosik, K.S. (1992). Suppression of MAP2 in cultured cerebellar macroneurons inhibits minor neurite formation. Neuron *9*, 607–618.

Callahan, C.A., and Thomas, J.B. (1994). Tau-beta-galactosidase, an axon-targeted fusion protein. Proc. Natl. Acad. Sci. USA *91*, 5972–5976.

Cambiazo, V., Gonzalez, M., and Maccioni, R.B. (1995). DMAP 85: a tau like protein from Drosophila melanogaster larvae. J. Neurochem. *64*, 1288–1297.

Canal, I., and Ferrús, A. (1986). The pattern of early neuronal differentiation in Drosophila melanogaster. J. Neurogenet. *3*, 293–319.

DiTella, M.C., Feiguin, F., Carri, N., Kosik, K.S., and Caceres, A. (1996). MAP 1B/TAU functional redundancy during laminin enhanced axonal growth. J. Cell Sci. *109*, 467–477.

Dotti, C.G., Banker, G.A., and Binder, L.I. (1987). The expression and distribution of the microtubule associated proteins tau and microtubule associated protein 2 in hippocampal neurons in the rat in situ and in cell culture. Neuroscience *23*, 121–130.

Dunin-Borkowski, O.M., and Brown, N.H. (1995). Mammalian CD2 is an effective heterologous marker of the cell surface in Drosophila. Dev. Biol. *168*, 689–693.

Edelmann, W., Zervas, M., Costello, P., Roback, L., Fischer, I., Hammarback, J.A., Cowan, N., Davies, P., Wainer, B., and Kucherlapati, R. (1996). Neuronal abnormalities in microtubule associated protein 1B mutant mice. Proc. Natl. Acad. Sci. USA *93*, 1270–1275.

Estes, P.S., Roos, J., van der Bliek, A., Kelly, R.B., Krishnan, K.S., and Ramaswami, M. (1996). Traffic of dynamin within individual Drosophila synaptic boutons relative to compartment specific markers. J. Neurosci. *16*, 5443–5456.

Fink, J.K., Jones, S.M., Esposito, C., and Wilkowski, J. (1996). Human microtubule associated protein 1a (MAP1A) gene: genomic organization, cDNA sequence, and developmental and tissue specific expression. Genomics *35*, 577–585.

Fujita, S.C., Zipursky, S.L., Benzer, S., Ferrus, A., and Shotwell, S.L. (1982). Monoclonal antibodies against the Drosophila nervous system. Proc. Natl. Acad. Sci. USA *79*, 7929–7933.

Giesen, K., Hummel, T., Stollewerk, A., Harrison, S., Travers, A., and Klämbt, C. (1997). Glial development in the Drosophila CNS requires concomitant activation of glial and repression of neuronal differentiation genes. Development *124*, 2307–2316.

Gindhart, J.G., Jr., Desai, C.J., Beushausen, S., Zinn, K., and Goldstein, L.S. (1998). Kinesin light chains are essential for axonal transport in Drosophila. J. Cell Biol. *141*, 443–454.

Goldstein, L.S., Laymon, R.A., and McIntosh, J.R. (1986). A microtubule associated protein in Drosophila melanogaster: identification,

characterization, and isolation of coding sequences. J. Cell Biol. *102*, 2076–2087.

Goodman, C.S., Bastiani, M.J., Doe, C.Q., du Lac, S., Helfand, S.L., Kuwada, J.Y., and Thomas, J.B. (1984). Cell recognition during neuronal development. Science *225*, 1271–1279.

Gordon-Weeks, P.R., and Fischer, I. (2000). MAP1B expression and microtubule stability in growing and regenerating axons. Microsc. Res. Tech. *48*, 63–74.

Hammarback, J.A., Obar, R.A., Hughes, S.M., and Vallee, R.B. (1991). MAP1B is encoded as a polyprotein that is processed to form a complex N terminal microtubule binding domain. Neuron *7*, 129–139.

Harada, A., Oguchi, K., Okabe, S., Kuno, J., Terada, S., Ohshima, T., Sato-Yoshitake, R., Takei, Y., Noda, T., and Hirokawa, N. (1994). Altered microtubule organization in small calibre axons of mice lacking tau protein. Nature *369*, 488–491.

Hirokawa, N. (1998). Kinesin and dynein superfamily proteins and the mechanism of organelle transport. Science *279*, 519–526.

Hoch, M., Broadie, K., Jackle, H., and Skaer, H. (1994). Sequential fates in a single cell are established by the neurogenic cascade in the Malpighian tubules of Drosophila. Development *120*, 3439–3450.

Hummel, T., Schimmelpfeng, K., and Klämbt, C. (1997). Fast and efficient egg collection and antibody staining from large numbers of *Drosophila* strains. DEG *207*, 131–135.

Hurd, D.D., and Saxton, W.M. (1996). Kinesin mutations cause motor neuron disease phenotypes by disrupting fast axonal transport in Drosophila. Genetics *144*, 1075–1085.

Irminger-Finger, I., Laymon, R.A., and Goldstein, L.S. (1990). Analysis of the primary sequence and microtubule binding region of the Drosophila 205K MAP. J. Cell Biol. *111*, 2563–2572.

Ito, K., Sass, H., Urban, J., Hofbauer, A., and Schneuwly, S. (1997). GAL4 responsive UAS tau as a tool for studying the anatomy and development of the Drosophila central nervous system. Cell Tissue Res. *290*, 1–10.

Kania, A., Salzberg, A., Bhat, M., D'Evelyn, D., He, Y., Kiss, I., and Bellen, H.J. (1995). P element mutations affecting embryonic peripheral nervous system development in Drosophila melanogaster. Genetics *139*, 1663–1678.

Kirkpatrick, L.L., and Brady, S.T. (1994). Modulation of the axonal microtubule cytoskeleton by myelinating Schwann cells. J. Neurosci. *14*, 7440–7450.

Klaes, A., Menne, T., Stollewerk, A., Scholz, H., and Klämbt, C. (1994). The Ets transcription factors encoded by the Drosophila gene pointed direct glial cell differentiation in the embryonic CNS. Cell *78*, 149–160.

Kosik, K.S., and Finch, E.A. (1987). MAP2 and tau segregate into dendritic and axonal domains after the elaboration of morphologically distinct neurites: an immunocytochemical study of cultured rat cerebrum. J. Neurosci. *7*, 3142–3153.

Kutschera, W., Zauner, W., Wiche, G., and Propst, F. (1998). The mouse and rat MAP1B genes: genomic organization and alternative transcription. Genomics *49*, 430–436.

Landon, M. (1977). Cleavage at aspartyl-prolyl bonds. Methods Enzymol. *47*, 145–149.

Langkopf, A., Hammarback, J.A., Muller, R., Vallee, R.B., and Garner, C.C. (1992). Microtubule associated proteins 1A and LC2. Two proteins encoded in one messenger RNA. J. Biol. Chem. *267*, 16561–16566.

Lien, L.L., Feener, C.A., Fischbach, N., and Kunkel, L.M. (1994). Cloning of human microtubule associated protein 1B and the identification of a related gene on chromosome 15. Genomics *22*, 273–280.

Mack, T.G., Koester, M.P., and Pollerberg, G.E. (2000). The microtubule-associated protein MAP1B is involved in local stabilization of turning growth cones. Mol. Cell. Neurosci. *15*, 51–65.

Matus, A. (1991). Microtubule associated proteins and neuronal morphogenesis. J. Cell Sci. *15 (suppl.)*, 61–67.

Matus, A., Bernhardt, R., and Hugh-Jones, T. (1981). High molecular weight microtubule associated proteins are preferentially associated with dendritic microtubules in brain. Proc. Natl. Acad. Sci. USA *78*, 3010–3014.

Noble, M., Lewis, S.A., and Cowan, N.J. (1989). The microtubule binding domain of microtubule associated protein MAP1B contains a repeated sequence motif unrelated to that of MAP2 and tau. J. Cell Biol. *109*, 3367–3376.

Peng, I., Binder, L.I., and Black, M.M. (1986). Biochemical and immunological analyses of cytoskeletal domains of neurons. J. Cell Biol. *102*, 252–262.

Pereira, A., Doshen, J., Tanaka, E., and Goldstein, L.S. (1992). Genetic analysis of a Drosophila microtubule associated protein. J. Cell Biol. *116*, 377–383.

Phillis, R., Statton, D., Caruccio, P., and Murphey, R.K. (1996). Mutations in the 8 kDa dynein light chain gene disrupt sensory axon projections in the Drosophila imaginal CNS. Development *122*, 2955–2963.

Reichmuth, C., Becker, S., Benz, M., Debel, K., Reisch, D., Heimbeck, G., Hofbauer, A., Klagges, B., Pflugfelder, G.O., and Buchner, E. (1995). The sap47 gene of Drosophila melanogaster codes for a novel conserved neuronal protein associated with synaptic terminals. Mol. Brain Res. *32*, 45–54.

Robertson, H.M., Preston, C.R., Phillis, R.W., Johnson-Schlitz, D.M., Benz, W.K., and Engels, W.R. (1988). A stable source of P-element transposase in Drosophila melanogaster. Genetics *118*, 6341–6351.

Roos, J., Hummel, T., Ng, N., Klämbt, C., and Davis, G.W. (2000). *Drosophila* futch regulates synaptic microtubule organization and is necessary for synaptic growth. Neuron *26*, this issue, 371–382.

Rorth, P. (1996). A modular misexpression screen in Drosophila detecting tissue specific phenotypes. Proc. Natl. Acad. Sci. USA *93*, 12418–12422.

Rorth, P., Szabo, K., Bailey, A., Laverty, T., Rehm, J., Rubin, G.M., Weigmann, K., Milan, M., Benes, V., Ansorge, W., and Cohen, S.M. (1998). Systematic gain of function genetics in Drosophila. Development *125*, 1049–1057.

Salzberg, A., D'Evelyn, D., Schulze, K.L., Lee, J.K., Strumpf, D., Tsai, L., and Bellen, H.J. (1994). Mutations affecting the pattern of the PNS in Drosophila reveal novel aspects of neuronal development. Neuron *13*, 269–287.

Salzberg, A., Prokopenko, S.N., He, Y., Tsai, P., Pal, M., Maroy, P., Glover, D.M., Deak, P., and Bellen, H.J. (1997). P element insertion alleles of essential genes on the third chromosome of Drosophila melanogaster: mutations affecting embryonic PNS development. Genetics *147*, 1723–1741.

Saxton, W.M., Hicks, J., Goldstein, L.S., and Raff, E.C. (1991). Kinesin heavy chain is essential for viability and neuromuscular functions in Drosophila, but mutants show no defects in mitosis. Cell *64*, 1093–1102.

Schoenfeld, T.A., and Obar, R.A. (1994). Diverse distribution and function of fibrous microtubule associated proteins in the nervous system. Int. Rev. Cytol. *151*, 67–137.

Scholz, H., Sadlowski, E., Klaes, A., and Klämbt, C. (1997). Control of midline glia development in the embryonic Drosophila CNS. Mech. Dev. *64*, 137–151.

Shea, T.B., and Beermann, M.L. (1994). Respective roles of neurofilaments, microtubules, MAP1B, and tau in neurite outgrowth and stabilization. Mol. Biol. Cell *5*, 863–875.

Srinivasan, S., and Karr, T.L. (1995). Biochemical characterization of related microtubule proteins in Drosophila melanogaster and adult rat brain. Brain Res. *701*, 39–46.

Takei, Y., Kondo, S., Harada, A., Inomata, S., Noda, T., and Hirokawa, N. (1997). Delayed development of nervous system in mice homozygous for disrupted microtubule associated protein 1B (MAP1B) gene. J. Cell Biol. *137*, 1615–1626.

Tautz, D., and Pfeifle, C. (1989). A non-radioactive in situ hybridization method for the localization of specific RNAs in Drosophila embryos reveals translational control of the segmentation gene hunchback. Chromosoma *98*, 81–85.

Tissot, M., Gendre, N., Hawken, A., Stortkuhl, K.F., and Stocker, R.F. (1997). Larval chemosensory projections and invasion of adult afferents in the antennal lobe of Drosophila. J. Neurobiol. *32*, 281–297.

Tix, S., Minden, J.S., and Technau, G.M. (1989). Preexisting neuronal

pathways in the developing optic lobes of Drosophila. Development *105*, 739–746.

Tonge, D.A., Golding, J.P., and Gordon-Weeks, P.R. (1996). Expression of a developmentally regulated, phosphorylated isoform of microtubule associated protein 1B in sprouting and regenerating axons in vitro. Neuroscience *73*, 541–551.

van Vactor, D., Sink, H., Fambrough, D., Tsoo, R., and Goodman, C.S. (1993). Genes that control neuromuscular specificity in Drosophila. Cell *73*, 1137–1153.

Veeranna, Amin, N.D., Ahn, N.G., Jaffe, H., Winters, C.A., Grant, P., and Pant, H.C. (1998). Mitogen activated protein kinases (Erk1,2) phosphorylate Lys Ser Pro (KSP) repeats in neurofilament proteins NF H and NF M. J. Neurosci. *18*, 4008–4021.

Wandosell, F., and Avila, J. (1987). Microtubule associated proteins present in different developmental stages of Drosophila melanogaster. J. Cell. Biochem. *35*, 83–92.

Zauner, W., Kratz, J., Staunton, J., Feick, P., and Wiche, G. (1992). Identification of two distinct microtubule binding domains on recombinant rat MAP 1B. Eur. J. Cell Biol. *57*, 66–74.

Zipursky, S.L., Venkatesh, T.R., Teplow, D.B., and Benzer, S. (1984). Neuronal development in the Drosophila retina: monoclonal antibodies as molecular probes. Cell *36*, 15–26.

GenBank Accession Number

The GenBank accession number for the *futsch* gene reported in this paper is CAA20006.